

# Controlling Radical Formation in the Photoactive Yellow Protein Chromophore\*\*

Ciarán R. S. Mooney, Michael A. Parkes, Andreas Iskra, and Helen H. Fielding\*

**Abstract:** To understand how photoactive proteins function, it is necessary to understand the photoresponse of the chromophore. Photoactive yellow protein (PYP) is a prototypical signaling protein. Blue light triggers *trans*–*cis* isomerization of the chromophore covalently bound within PYP as the first step in a photocycle that results in the host bacterium moving away from potentially harmful light. At higher energies, photoabsorption has the potential to create radicals and free electrons; however, this process is largely unexplored. Here, we use photoelectron spectroscopy and quantum chemistry calculations to show that the molecular structure and conformation of the isolated PYP chromophore can be exploited to control the competition between *trans*–*cis* isomerization and radical formation. We also find evidence to suggest that one of the roles of the protein is to impede radical formation in PYP by preventing torsional motion in the electronic ground state of the chromophore.

In nature, light drives many important processes such as photosynthesis, vision, and phototaxis. At the heart of all these processes is a small chromophore whose photochemical response initiates large-scale conformational changes in the protein wrapped around it, which in turn leads to a response at the cellular level. In addition to the desired photochemical reaction pathway, molecular chromophores are subject to competing processes such as internal conversion (IC), intersystem crossing, and intramolecular vibrational redistribution and, in photoactive proteins in which the chromophore exists in a deprotonated anionic form, electron emission.<sup>[1–4]</sup> The

role of the protein in controlling the competition between these processes is still not understood fully.

PYP is the primary photoreceptor for the negative photoactive response of the *Halorhodospira halophila* bacterium to the potentially harmful effects of blue light and has been the subject of numerous experimental and theoretical studies as a model photoreceptor.<sup>[5–8]</sup> The chromophore of PYP is derived from *trans* *para*-coumaric acid (*p*CA) and exists in its deprotonated phenoxide form (*p*CA<sup>−</sup>) in the ground electronic state (Figure 1). Numerous gas-phase

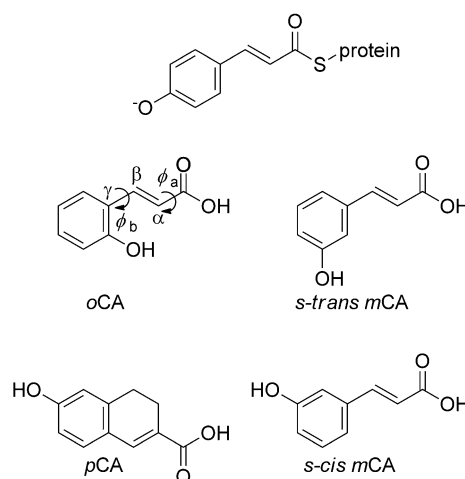


**Figure 1.** Structures of the PYP chromophore in the protein (top) and those employed in this work. The conformation of *o*CA around the bond linking the  $\beta$  and  $\gamma$  atoms is well-defined, but for *m*CA it is undefined and exists in both *s*-*cis* and *s*-*trans* conformations, where *s*-*cis* and *s*-*trans* define the position of the phenol OH group with respect to the  $\beta$  hydrogen. As drawn,  $\phi_a = 0^\circ$ .

studies of isolated model PYP chromophores have shown that the protein environment does not influence the absorption spectrum significantly but, following excitation around 400 nm, it plays a key role in directing *trans*–*cis* isomerization of the chromophore and impeding electron emission and radical formation.<sup>[9–18]</sup> Electron emission has also been observed following excitation at shorter wavelengths in PYP<sup>[1,2]</sup> and in isolated PYP chromophores in solution,<sup>[19]</sup> although the photoresponse of the isolated chromophore in vacuum at short wavelengths is largely unexplored.

Here, we use anion photoelectron spectroscopy<sup>[20–22]</sup> and quantum chemistry calculations to investigate the effect of molecular structure on the competition between IC and electron emission following 364–315 nm excitation of deprotonated anions derived from *p*CA and two of its isomers, *trans* *ortho*-coumaric acid (*o*CA) and *trans* *meta*-coumaric acid

[\*] C. R. S. Mooney, M. A. Parkes, H. H. Fielding  
Department of Chemistry, University College London  
20 Gordon Street, London WC1H 0AJ (UK)  
E-mail: h.h.fielding@ucl.ac.uk

A. Iskra  
Current address:  
Physical and Theoretical Chemistry Laboratory  
University of Oxford  
South Parks Road, Oxford OX1 3QZ (UK)

[\*\*] This work was supported by EPSRC grants (grant numbers EP/L005646/1 and EP/D054508/1). We acknowledge use of the EPSRC UK National Service for Computational Chemistry Software (NSCCS) at Imperial College London and discussions with Alexandra Simperler, and the iOpenShell Center for Computational Studies of Electronic Structure and Spectroscopy of Open-Shell and Electronically Excited Species, supported by the National Science Foundation. We are grateful to Christopher West and Jan Verlet (Durham) who enabled us to record preliminary data using their anion photoelectron spectrometer.

Supporting information for this article is available on the WWW under <http://dx.doi.org/10.1002/anie.201500549>.

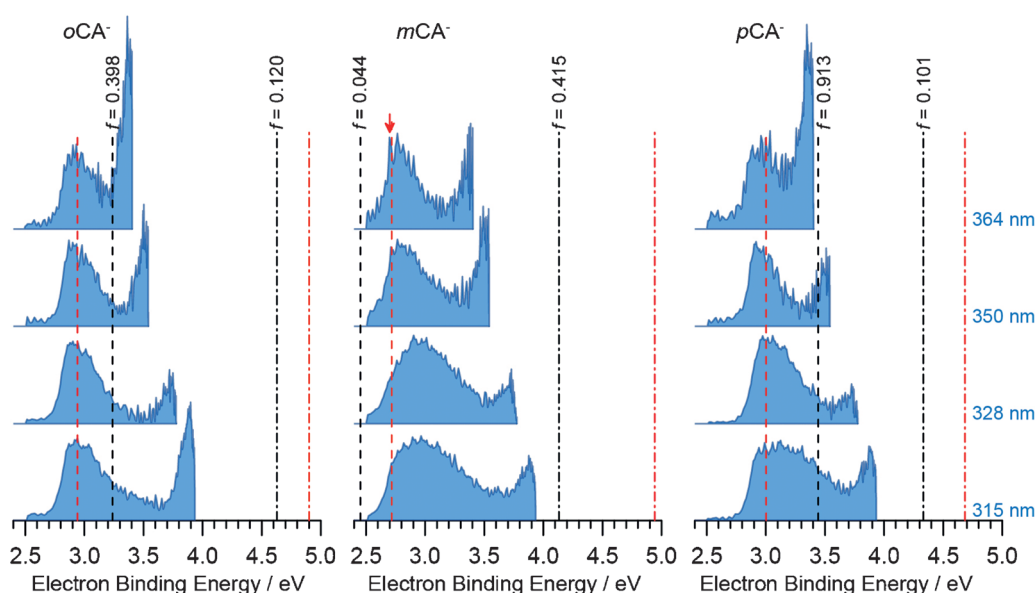


**Figure 2.** Photoelectron spectra of  $oCA^-$ ,  $mCA^-$  and  $pCA^-$  recorded at 364 nm (3.41 eV), 350 nm (3.54 eV), 328 nm (3.78 eV) and 315 nm (3.94 eV), plotted as a function of eBE. Spectra have been normalized to the maxima of the low eBE features. Vertical red lines mark the VDEs calculated for the lowest energy (planar) configurations of the chromophores in their phenolate (dashed) and carboxylate (dot-dashed) forms. The vertical red arrow marks the position of the peak at  $2.70 \pm 0.05$  eV in the 364 nm spectrum of  $mCA^-$  (see text). Vertical black lines mark the calculated VEEs (with oscillator strengths,  $f$ ) of the  $1^1\pi\pi^*$  (dashed) and  $2^1\pi\pi^*$  (dot-dashed) states of the phenolate forms of the anions in their lowest energy (planar) configurations.

( $mCA$ ) (Figure 1). Photoelectron spectra of  $oCA^-$ ,  $mCA^-$  and  $pCA^-$  are recorded as a function of electron kinetic energy (eKE) and presented in Figure 2 as a function of electron binding energy,  $eBE = h\nu - eKE$ . All the spectra have similar profiles: a broad feature at low eBE and a sharp feature at high eBE.

The maxima of the broad features remain at constant eBE for all photon energies, signifying a direct photodetachment (PD) process. The maxima of these features are close to the vertical detachment energies (VDEs) we calculated for the phenolate forms of the chromophores (2.7–3.0 eV), which are about 2 eV lower than those calculated for the carboxylate forms (4.7–4.9 eV; Figure 2). Thus, our measurements support earlier suggestions that the coumaric acid chromophores are formed in their phenolate forms during the electrospray-ionization process.<sup>[13,17]</sup>

For  $mCA^-$  and  $pCA^-$ , the broad features change shape on their high eBE side as the photon energy is increased. This can be explained in terms of resonant excitation of the  $2^1\pi\pi^*$  states (calculated VEEs around 4.2 and 4.3 eV for  $mCA^-$  and  $pCA^-$ , respectively) followed by autodetachment, that is, indirect PD (Figure 3). A similar effect was observed in photoelectron spectra of the deprotonated green fluorescent protein (GFP) chromophore anion following resonant excitation of the  $2^1\pi\pi^*$  state.<sup>[22]</sup> For  $oCA^-$ , the broad feature does not change shape, which is consistent with the  $2^1\pi\pi^*$  state lying higher in energy (calculated VEE of about 4.6 eV) and suggests that it is inaccessible at these photon energies.

The sharp features shift to higher eBE with increasing photon energy, signifying an indirect electron emission process. PD from  $1^1\pi\pi^*$  and thermionic emission (TE) from

the vibrationally hot ground electronic state of the anion are possible electron emission pathways (Figure 3). The exponential profile is characteristic of TE. Similar features have been observed in photoelectron spectra of other molecular anions, such as the *p*-benzoquinone radical anion,<sup>[23]</sup> and deprotonated GFP chromophore anion,<sup>[24]</sup> and, moreover, TE from a hot ground state is consistent with IC back to the ground electronic state, which has been observed to occur on a 52 ps timescale in methyl-terminated (ketone)  $pCA^-$  following photoexcitation of  $S_1$  at 3.1 eV.<sup>[10]</sup>

The vertical excitation energies (VEEs) of

the  $1^1\pi\pi^*$  states in  $oCA^-$  and  $pCA^-$  have large oscillator strengths and are close to the lowest photon energy (Figure 2). Thus, the 3.41 eV photoelectron spectra of  $oCA^-$  and  $pCA^-$  are dominated by low eKE photoelectrons arising from indirect PD from the  $1^1\pi\pi^*$  state and TE from  $S_0$  (Figure 3). In contrast, the VEE of the  $1^1\pi\pi^*$  state in  $mCA^-$  is much lower in energy and weaker and, consequently, the

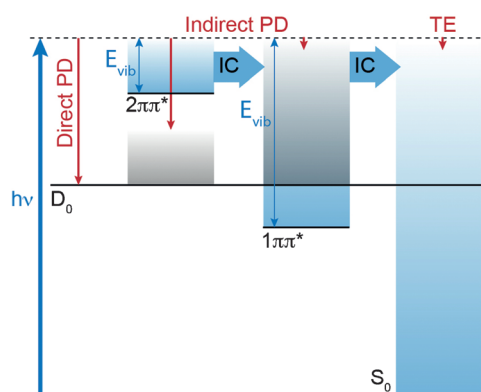


**Figure 3.** Schematic diagram illustrating electron emission processes (red arrows) following photoexcitation ( $h\nu$ ). Direct photodetachment (PD) gives photoelectrons with maximum eKE around  $h\nu - E(D_0 - S_0)$ . Resonant excitation of the  $2^1\pi\pi^*$  state with excess vibrational energy  $E_{vib} = h\nu - E(2^1\pi\pi^* - S_0)$  (blue shading) may be followed by indirect PD generating electrons with eKE around  $E_{PD} = E(2^1\pi\pi^* - D_0)$ , as a result of the propensity for conserving vibrational energy during the detachment process (grey shading), or by IC to  $1^1\pi\pi^*$ , followed by indirect PD or IC to  $S_0$ . Subsequent statistical TE from  $S_0$  is characterized by electrons with eKE about 0 eV.

3.41 eV photoelectron spectrum of  $mCA^-$  is dominated by direct PD (Figure 3).

The  $S_0 \rightarrow 1^1\pi\pi^*$  transitions are all dominated by transitions from the highest occupied molecular orbitals (HOMOs) (Figure 4). For  $oCA^-$  and  $pCA^-$ , the HOMOs are delocalized across the whole molecule with  $\pi$  bonding character across the C=C double bond between the phenoxide and carboxylic

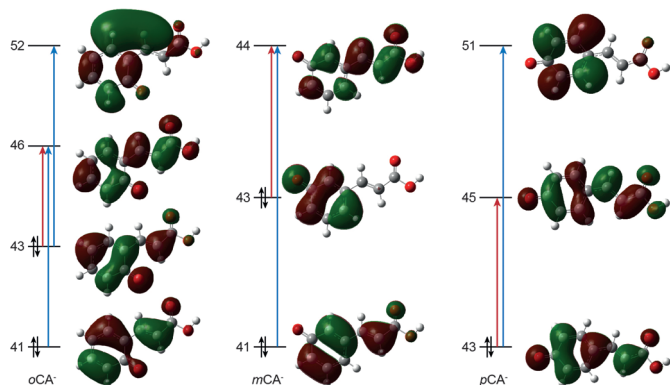


**Figure 4.** Main ground-state molecular orbitals involved in the  $1^1\pi\pi^*$  and  $2^1\pi\pi^*$  transitions for  $oCA^-$ ,  $s$ -cis  $mCA^-$ , and  $pCA^-$ .

acid groups, whereas for  $mCA^-$  the HOMO is a pair of out-of-phase  $\pi$  orbitals on the phenoxide moiety and there is negligible electron density on the propenoic acid moiety. The  $S_0 \rightarrow 1^1\pi\pi^*$  transitions in  $oCA^-$  and  $pCA^-$  are dominated by  $\pi \rightarrow \pi^*$  transitions on the C=C double bond and the  $S_0 \rightarrow 1^1\pi\pi^*$  transition in  $mCA^-$  involves  $\pi \rightarrow \pi^*$  transitions on the phenoxide group and charge transfer to the propenoic acid moiety. Thus, moving the position of the  $O^-$  group on the phenoxide moiety provides a means of controlling the conjugation, which in turn controls the competition between resonant excitation of the  $1^1\pi\pi^*$  state and direct detachment.

Since the  $mCA^-$  photoelectron spectrum is dominated by direct PD, it can be modelled by calculating the Franck-Condon overlap between the ground electronic states of the anion and the neutral radical (Figure 5). The excellent agreement between the calculated and experimental spectra allows us to assign the well-resolved feature in the experimental photoelectron spectrum at  $2.70 \pm 0.05$  eV to the 0-0 transition (2.71 eV) and tells us that the adiabatic detachment energy is equivalent to the VDE. We also determine that the photoelectron spectrum is dominated by a progression in the  $\nu_{11}$  mode (harmonic frequency  $531\text{ cm}^{-1}$ ) corresponding to an in-plane vibration (Figure 5).

Curiously, the  $oCA^-$  and  $pCA^-$  photoelectron spectra reveal significant photoemission at lower eBEs than the calculated VDEs (Figure 2). Rotation around the single bond between the C=C double bond and the phenoxide group has been shown to facilitate *trans*-*cis* isomerization in PYP.<sup>[9,25]</sup> In Figure 6, the 3.41 eV (364 nm) experimental photoelectron spectrum for  $pCA^-$  is shown together with the positions of the calculated VDEs for the deprotonated chromophore anion in its optimized planar geometry and geometries optimized with  $\phi_a = 90^\circ$  or  $\phi_b = 90^\circ$ .

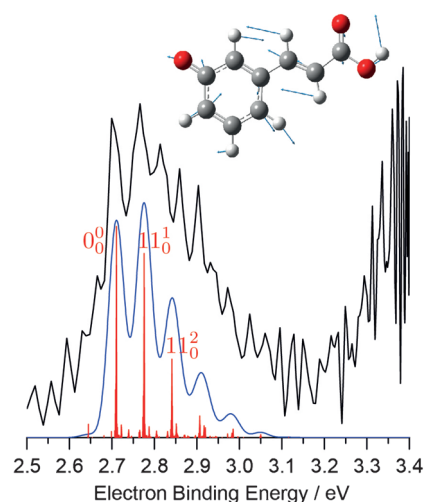


**Figure 5.** Calculated photoelectron stick spectrum of the phenolate form of the deprotonated  $s$ -cis  $mCA^-$  chromophore at  $T = 300\text{ K}$  (red) and stick spectrum convoluted with Gaussian instrument profiles with half-width at half-maximum of 18 meV (blue) compared with the experimental 364 nm (3.41 eV) photoelectron spectrum (black). Inset: Atomic displacement vectors of the dominant  $\nu_{11}$  normal mode of the neutral radical.

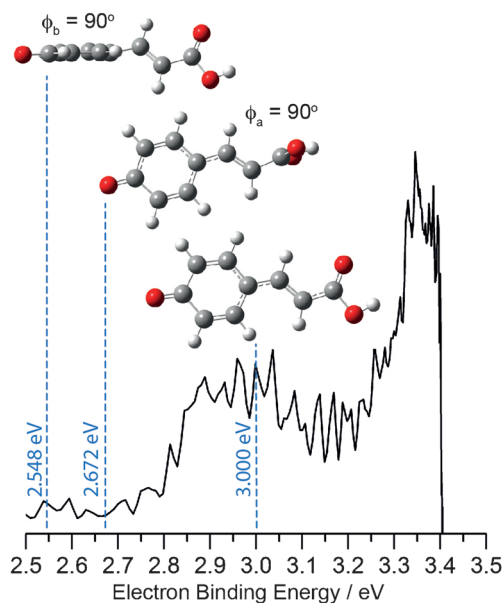


**Figure 6.** 3.41 eV (364 nm) photoelectron spectrum of the phenolate form of the deprotonated  $pCA^-$  chromophore shown with calculated VDEs for the minimum energy geometry and geometries optimized with  $\phi_a = 90^\circ$  and  $\phi_b = 90^\circ$ .

The substantial photoelectron signal lying below the VDE for the planar chromophore lies above the VDEs for the  $90^\circ$  twisted chromophores and therefore we attribute the photoelectron signal below the VDE for the planar chromophore to PD from twisted chromophore anions. This suggests that one of the reasons the protein environment in PYP restricts torsional motion in the ground electronic state of the anion is to raise the threshold for direct PD and thus impede electron emission and radical formation. Hydrogen bonding between

the O<sup>−</sup> on the phenoxide group and the  $\alpha$  hydrogen in *o*CA<sup>−</sup> is likely to restrict rotation around  $\phi_b$ , perhaps explaining why the photoemission at lower eBEs is less significant than for *p*CA<sup>−</sup>.

At the highest photon energy (3.94 eV), the contribution from low eKE electrons increases, most noticeably for *o*CA<sup>−</sup>. This could be attributed to detachment to higher lying continua or access to a new conical intersection providing an efficient radiationless decay path back to S<sub>0</sub>. Unravelling the decay pathway will require femtosecond time-resolved photoelectron spectroscopy measurements,<sup>[26–28]</sup> which are currently underway in our laboratory.

In summary, we have studied the competition between electron emission and internal conversion in the model PYP chromophore, *p*CA<sup>−</sup>, and two of its isomers. We show that moving the position of the O<sup>−</sup> group on the phenoxide moiety of the chromophore changes the branching ratio between direct PD and resonant excitation of <sup>1</sup> $\pi\pi^*$  and <sup>2</sup> $\pi\pi^*$  states, which subsequently undergo IC to lower electronic states followed by autodetachment or TE. We also show that torsional motions in the ground electronic state are responsible for lowering the VDE, suggesting that one of the reasons the protein maintains the planarity of the chromophore in its ground electronic state is to impede electron emission and radical formation. These results illustrate how modifications to the chemical structure away from the excited state reaction coordinate can control the competition between dynamics on the excited state and radical formation and demonstrate the importance of low-frequency single bond rotations.

**Keywords:** biophysics · chromophores · photochemistry · proteins · radical formation

**How to cite:** *Angew. Chem. Int. Ed.* **2015**, *54*, 5646–5649  
*Angew. Chem.* **2015**, *127*, 5738–5741

- [1] D. S. Larsen, I. H. M. van Stokkum, M. Vengris, M. A. van der Horst, F. L. de Weerd, K. J. Hellingwerf, R. van Grondelle, *Biophys. J.* **2004**, *87*, 1858–1872.
- [2] J. Zhu, L. Paparelli, M. Hospes, J. Arents, J. T. M. Kennis, I. H. M. Van Stokkum, K. J. Hellingwerf, M. L. Groot, *J. Phys. Chem. B* **2013**, *117*, 11042–11048.
- [3] A. M. Bogdanov, A. S. Mishin, I. V. Yampolsky, V. V. Belousov, D. M. Chudakov, F. V. Subach, V. V. Verkhusha, S. Lukyanov, K. A. Lukyanov, *Nat. Chem. Biol.* **2009**, *5*, 459–461.
- [4] K. M. Solntsev, D. Ghosh, A. Amador, M. Josowicz, A. I. Krylov, *J. Phys. Chem. Lett.* **2011**, *2*, 2593–2597.
- [5] T. E. Meyer, *Biochim. Biophys. Acta* **1985**, *806*, 175–183.
- [6] W. W. Sprenger, W. D. Hoff, J. P. Armitage, K. J. Hellingwerf, *J. Bacteriol.* **1993**, *175*, 3096–3104.
- [7] K. J. Hellingwerf, J. Hendriks, T. Gensch, *J. Phys. Chem. A* **2003**, *107*, 1082–1094.
- [8] F. Schotte, H. S. Cho, V. R. I. Kaila, H. Kamikubo, N. Dashdorj, E. R. Henry, T. J. Graber, R. Henning, M. Wulff, G. Hummer, M. Kataoka, P. A. Anfinrud, *Proc. Natl. Acad. Sci. USA* **2012**, *109*, 19256–19261.
- [9] G. Groenhof, M. Bouxin-Cademartory, B. Hess, S. P. de Visser, H. J. C. Berendsen, M. Olivucci, A. E. Mark, M. A. Robb, *J. Am. Chem. Soc.* **2004**, *126*, 4228–4233.
- [10] I.-R. Lee, W. Lee, A. H. Zewail, *Proc. Natl. Acad. Sci. USA* **2006**, *103*, 258–262.
- [11] L. Lammich, J. Rajput, L. H. Andersen, *Phys. Rev. E* **2008**, *78*, 051916.
- [12] M. de Groot, E. V. Gromov, H. Koppel, W. J. Buma, *J. Phys. Chem. B* **2008**, *112*, 4427–4434.
- [13] T. Rocha-Rinza, O. Christiansen, J. Rajput, A. Gopalan, D. B. Rahbek, L. H. Andersen, A. V. Bochenkova, A. A. Granovsky, K. B. Bravaya, A. V. Nemukhin, K. L. Christiansen, M. B. Nielsen, *J. Phys. Chem. A* **2009**, *113*, 9442–9449.
- [14] T. Rocha-Rinza, O. Christiansen, D. B. Rahbek, B. Klærke, L. H. Andersen, K. Lincke, M. B. Nielsen, *Chem. Eur. J.* **2010**, *16*, 11977–11984.
- [15] S. Smolarek, A. Vdovin, D. L. Perrier, J. P. Smit, M. Drabbels, W. J. Buma, *J. Am. Chem. Soc.* **2010**, *132*, 6315–6317.
- [16] S. Smolarek, A. Vdovin, E. M. M. Tan, M. de Groot, W. J. Buma, *Phys. Chem. Chem. Phys.* **2011**, *13*, 4393–4399.
- [17] D. Zuev, K. B. Bravaya, T. D. Crawford, R. Lindh, A. I. Krylov, *J. Chem. Phys.* **2011**, *134*, 034310.
- [18] M. Uppsten, B. Durbeej, *J. Comput. Chem.* **2012**, *33*, 1892–1901.
- [19] D. S. Larsen, M. Vengris, I. H. M. van Stokkum, M. a. van der Horst, F. L. de Weerd, K. J. Hellingwerf, R. van Grondelle, *Biophys. J.* **2004**, *86*, 2538–2550.
- [20] A. R. McKay, M. E. Sanz, C. R. S. Mooney, R. S. Minns, E. M. Gill, H. H. Fielding, *Rev. Sci. Instrum.* **2010**, *81*, 123101.
- [21] C. R. S. Mooney, M. E. Sanz, A. R. McKay, R. J. Fitzmaurice, A. E. Aliev, S. Caddick, H. H. Fielding, *J. Phys. Chem. A* **2012**, *116*, 7943–7949.
- [22] C. R. S. Mooney, M. A. Parkes, L. Zhang, H. C. Hailes, A. Simperler, M. J. Bearpark, H. H. Fielding, *J. Chem. Phys.* **2014**, *140*, 205103.
- [23] D. A. Horke, Q. Li, L. Blancafort, J. R. R. Verlet, *Nat. Chem.* **2013**, *5*, 711–717.
- [24] C. W. West, A. S. Hudson, S. L. Cobb, J. R. R. Verlet, *J. Chem. Phys.* **2013**, *139*, 071104.
- [25] A. D. Stahl, M. Hospes, K. Singhal, I. van Stokkum, R. van Grondelle, M. L. Groot, K. J. Hellingwerf, *Biophys. J.* **2011**, *101*, 1184–1192.
- [26] R. S. Minns, D. S. N. Parker, T. J. Penfold, G. A. Worth, H. H. Fielding, *Phys. Chem. Chem. Phys.* **2010**, *12*, 15607–15615.
- [27] R. Spesyvtsev, O. M. Kirkby, M. Vacher, H. H. Fielding, *Phys. Chem. Chem. Phys.* **2012**, *14*, 9942–9947.
- [28] C. R. S. Mooney, D. A. Horke, A. S. Chatterley, A. Simperler, H. H. Fielding, J. R. R. Verlet, *Chem. Sci.* **2013**, *4*, 921.

Received: February 24, 2015

Published online: March 17, 2015